Tie-Simplex Based Compositional Space Parameterization: Continuity and Generalization to Multiphase Systems

Alireza Iranshahr, Denis V. Voskov, and Hamdi A. Tchelepi
Dept. of Energy Resources Engineering, Stanford University, Stanford, CA 94305

DOI 10.1002/aic.13919
Published online September 25, 2012 in Wiley Online Library (wileyonlinelibrary.com).

A theoretical analysis is provided of the continuity of multiphase compositional space parameterization for thermal-compositional reservoir simulation. It is shown that the tie-simplex space changes continuously as a function of composition, pressure, and temperature, and this justifies the Compositional Space Adaptive Tabulation (CSAT) framework, in which a discrete number of tie-simplexes are constructed, tabulated, and reused in the course of a simulation. The CSAT is extended for thermal-compositional displacements for mixtures that can form an arbitrary number of phases. In particular, the construction is described of three-phase tie-simplex tables, and it is shown how the degeneration of multiphase regions can be accurately captured over wide ranges of temperature and pressure. Several challenging multiphase examples are used to demonstrate the accuracy and effectiveness of phase-state identification using tabulated tie-simplexes. © 2012 American Institute of Chemical Engineers *AIChE J,* 59: 1684–1701, 2013
Keywords: phase equilibrium, numerical solution, thermodynamics/classical, multiphase flow, petroleum

Introduction

Thermal and gas injection processes are among the most commonly used techniques to improve oil recovery. To obtain reliable predictions based on the numerical simulation of such processes, a thermal-compositional model is used, where the partial differential equations of the conservation of mass, energy, and momentum are solved together with the equations of thermodynamic equilibrium.[1]

Coupling thermodynamics with the conservation equations is a major challenge in the development of a general-purpose thermal-compositional simulation framework. The partial differential equations are highly nonlinear, and they are tightly coupled to the phase equilibrium relations. To deal with thermal-compositional models of practical utility, accurate treatment of the thermodynamic phase behavior is crucial.[2] Moreover, in many displacement processes, a large number of components partition among more than two fluid phases. This is common in steam injection problems and in mixtures that include CO_2 or sour gas over wide ranges of temperature and pressure. Modeling the phase behavior of such systems is challenging even when all the phases are immiscible with each other. The complexity of the problem increases when multiphase regions approach the critical state.

Simplified compositional (or modified black-oil) models have been developed in order to account for the thermodynamic phase behavior in reservoir flow simulation.[3,4] One of the most common approaches is the so-called "constant *K*-values" method, where it is assumed that the component equilibrium factors, *K*-values, are functions of temperature and pressure only, and therefore, the thermodynamic equilibrium can be modeled efficiently using tables of *K*-values (see Aziz et al.[5] for a practical example). However, the accuracy of the constant *K*-values approach is limited to immiscible displacements at relatively low pressure, where the assumption of composition-independent *K*-values is valid. Limited-compositional models can be thermodynamically inconsistent, or inaccurate.[6] Consequently, such models may not be able to capture the complex physics in problems involving development of miscibility, or interactions involving more than two fluid phases. In this work, we use an Equation of State (EoS) method to represent the phase behavior associated with thermal-compositional flow simulation.

Phase equilibrium calculations can be the most expensive kernel in a compositional flow simulation. Given an overall composition at some pressure and temperature conditions, the number of phases and their compositions must be determined for every control volume (gridblock) at each time step. The conventional approach is based on: (1) performing a phase-stability test for single-phase gridblocks[7] and (2) solving the fugacity constraints[8] together with the coupled nonlinear flow equations for gridblocks that have more than one phase. Robust algorithms for stand-alone calculations of multiphase stability and flash procedures have been described by several authors (see Michelsen and Mollerup[9] for instance). However, previous developments for phase behavior computations coupled with flow and transport have basically focused on methodologies that are suitable for only two-phase compositional simulation. Modern approaches, such as bypassing of phase stability analysis, are presented recently for fast compositional calculations.[10]

To improve the computational performance and robustness of EoS-based phase behavior for two-phase compositional

Correspondence concerning this article should be addressed to A. Iranshahr at iranshahr@gmail.com.

simulation, a tie-line based Compositional Space Parameterization (CSP) framework has been developed.[11] An effective way of utilizing CSP for general-purpose simulation is the Compositional Space Adaptive Tabulation (CSAT) framework, in which tie-line parameterization is used to accelerate the convergence of EoS-based calculations.[12] CSAT is based on theoretical findings from the Method of Characteristics (MoC) solutions of gas injection problems under ideal assumptions.[13,14] The MoC solutions show that only a few (key) tie-lines determine the structure of the solution route in compositional space. The MoC-based theory has been recently extended to thermal[15] and three-phase[16,17] displacements.

CSAT constructs and tabulates tie-lines adaptively. The tie-line tables are then used to identify the phase-state of compositions encountered in the course of the simulation. Linear interpolation in pressure is performed to obtain a tie-line for a composition with the specified pressure value.[12]

The initial development of CSAT for immiscible displacements has been generalized for multi-contact miscible problems.[18] It is shown that adaptive tabulation of the critical tie-lines significantly improves the efficiency and accuracy of multi-contact miscible simulation. Generalization of CSAT to thermal problems, where tabulation and interpolation as a function of temperature and pressure are performed, has been presented by Iranshahr et al.[19] Extension to multiphase parameterization using tie-simplexes is described by Voskov and Tchelepi.[20] The wide range of examples presented in these references shows that CSAT is an effective method for phase behavior modeling in general-purpose compositional simulation.

To deal with multicomponent systems that can form more than two equilibrium phases, we assume that a nondegenerate *base tie-simplex parameterization* is associated with the compositional system of interest. The maximum number of phases, N_p^{max}, that can coexist for the base parameterization is assumed to be known in our developments. N_p^{max} is defined such that the extensions of N_p^{max}-phase tie-simplexes do not intersect inside the compositional space.[20,21] Moreover, N_p^{max} cannot be greater than the number of components in the system. As we will discuss further, with changes in temperature and pressure, multiphase regions in the base parameterization become critical (degenerate to lower-dimensional multiphase regions), or they disappear from the compositional space. So, we assume that no new multiphase region will appear with changes in the T–p conditions. If the assumed N_p^{max} is wrong, tie-simplexes will actually intersect *inside some multiphase regions* (see e.g., Voskov and Tchelepi[20]). In this case, the value of N_p^{max} must be increased, and the parameterization must be repeated.

The value of N_p^{max} is estimated based on the preliminary knowledge of the system (e.g., existing hydrocarbon components, temperature, and pressure conditions). Further studies include parameterization of the compositional space between injection and initial compositions across the practical range of temperature and pressure (determined from the initial, injection, and production conditions). These primitive studies lead to an initial estimate of N_p^{max}, which is used to perform actual reservoir flow simulation. For this purpose, CSAT constructs base parameterizations in multiphase tables (as we will discuss further). According to the practical T–p range, multiphase regions of the base parameterization might degenerate at further T–p levels of the table. If any tie-simplexes intersect inside the multiphase regions, the simulation studies are performed with the modified value of N_p^{max}.

In this work, we extend CSAT in two important directions. First, we provide a theoretical basis for the continuity of CSP in terms of tie-simplexes. The continuity of the tie-simplex space justifies the use of discrete tie-simplexes for flow simulation, where interpolation in pressure and temperature using a limited number of tie-simplexes is performed during a simulation run. Second, we extend CSAT to multiphase (more than two phases) systems. We focus on the complex behaviors of the tie-triangles and tie-lines associated with three-phase, steam-injection problems. The algorithms that capture the degeneration of the tie-triangles into tie-lines are described in detail. We also demonstrate how miscibility of oil and gas phases can be modeled in systems involving steam. Interpolation in the parameterized compositional space is used to identify the phase-state and proves to be as reliable as the "conventional" phase-stability test for three-phase mixtures. We demonstrate the effectiveness and accuracy of the framework using several compositional problems with complex behaviors.

Continuity of CSP

In this section, we prove the continuity of tie-simplex parameterization. The correct value of N_p^{max} is assumed to be known for the given thermodynamic system. Let

$$\mathbf{x}_j = \mathbf{x}_j(\mathbf{z}, T, p), \qquad j = 1, \ldots, M_p,$$

represent the endpoints of an M_p-phase tie-simplex ($2 \le M_p \le N_p^{max}$) calculated in a multi-stage negative-flash framework.[21] Continuity indicates that bounded changes in the parameters yield well-defined changes in tie-simplex compositions. Note that the phase-state of $\mathbf{z}$ may change with varying flash parameters; however, the parameterizing tie-simplexes will change continuously. These developments show the continuity of negative-flash in the multi-stage formulation described by Iranshahr et al.[21]

First, we study two-phase systems, and we show that at constant temperature and pressure, tie-line parameterization of a continuous trajectory in the compositional space is continuous. Moreover, the tie-line that parameterizes a given composition changes continuously with pressure and temperature. First, we assume that there is only one two-phase region in the compositional space ($N_p^{max} = 2$). In Appendix A, we show continuity for systems with $N_p^{max} > 2$.

Parameterization along a continuous path

We start with parameterizing a continuous path in compositional space at constant temperature and pressure. Assuming that both phases are at chemical equilibrium, we write the equality of chemical potentials for each component as

$$\mu_{i,1} = \mu_{i,2}, \qquad i = 1, \ldots, N_c. \tag{1}$$

Note that the chemical potential of component i in phase j, $\mu_{i,j}$, is a function of pressure, temperature, and the molar amounts of all the components present in that phase, so that

$$\mu_{i,j} = \mu_{i,j}(p, T, n_{1,j}, n_{2,j}, \ldots, n_{N_c,j}). \tag{2}$$

The overall molar composition of a component, z_i, is defined as

$$z_i = \frac{n_{i,\mathrm{tot}}}{\sum_{l=1}^{N_c} n_{l,\mathrm{tot}}}, \qquad i = 1, \ldots, N_c, \tag{3}$$

where $n_{i,\mathrm{tot}}$ represents the total molar amount of component i. Here, we assume that $0 < n_{i,\mathrm{tot}}$. Let ξ parameterize a continuous trajectory in compositional space, then along ξ, we have

$$\frac{dn_{i,\mathrm{tot}}}{d\xi} = \left(\frac{\partial n_{i,\mathrm{tot}}}{\partial \xi}\right)_{p,T,n_{k\neq i,\mathrm{tot}}}, \qquad i = 1,\ldots,N_c, \tag{4}$$

where the subscript $n_{k\neq i,\mathrm{tot}}$ indicates that the total molar amounts of all the components, k, except i are held fixed. Differentiating Eq. 3 with respect to ξ yields

$$\sum_{l=1}^{N_c}(\delta_{i,l} - z_i)\left(\frac{\partial n_{l,\mathrm{tot}}}{\partial \xi}\right)_{p,T,n_{k\neq l,\mathrm{tot}}} = \frac{dz_i}{d\xi}\sum_{l=1}^{N_c} n_{l,\mathrm{tot}}, \qquad i = 1,\ldots,N_c, \tag{5}$$

where δ represents the Kronecker delta. Therefore, if $(\partial n_{l,\mathrm{tot}}/\partial\xi)_{p,T,n_{k\neq l,\mathrm{tot}}}$ is bounded, then $dz_i/d\xi$ will also be bounded (Note that $0 < z_i < 1$, and $0 < \sum_{l=1}^{Nc} n_{l,\mathrm{tot}}$). Similar results can be derived for the compositions of each phase. As

$$\sum_{l=1}^{N_c}\frac{dz_l}{d\xi} = 0, \tag{6}$$

only a subset of $N_c - 1$ equations from Eq. 5 are linearly independent. As a result, there is not a unique set of changes in the molar amounts that corresponds to the given changes in the molar compositions. In the following, we assume a set of continuous changes in the total molar amounts of components that satisfies Eq. 5 for the given trajectory in compositional space. Here, we provide a formal proof for the first part of the Continuity Theorem.

Continuity Theorem, Part 1. *At constant temperature and pressure, tie-line parameterization of a continuous path in compositional space is continuous.*

Proof: First, we consider changes in the phase behavior along a continuous trajectory that is entirely inside the two-phase region. Differentiating Eq. 1 with respect to ξ at fixed pressure and temperature yields

$$\sum_{l=1}^{N_c}\left(\frac{\partial \mu_{i,1}}{\partial n_{l,1}}\cdot\frac{\partial n_{l,1}}{\partial \xi}\right)_{p,T,n_{k\neq l,1}} - \sum_{l=1}^{N_c}\left(\frac{\partial \mu_{i,2}}{\partial n_{l,2}}\cdot\frac{\partial n_{l,2}}{\partial \xi}\right)_{p,T,n_{k\neq l,2}} = 0, \qquad i = 1,\ldots,N_c. \tag{7}$$

Material balance for each component is

$$n_{i,\mathrm{tot}} = n_{i,1} + n_{i,2}, \qquad i = 1,\ldots,N_c. \tag{8}$$

Along the path, we differentiate Eq. 8 to obtain

$$\left(\frac{\partial n_{i,\mathrm{tot}}}{\partial \xi}\right)_{p,T,n_{k\neq i,\mathrm{tot}}} = \left(\frac{\partial n_{i,1}}{\partial \xi}\right)_{p,T,n_{k\neq i,1}} + \left(\frac{\partial n_{i,2}}{\partial \xi}\right)_{p,T,n_{k\neq i,2}}, \qquad i = 1,\ldots,N_c. \tag{9}$$

Combining Eqs. 7 and 9 yields

$$\sum_{l=1}^{N_c}[J^1_{i,l} + J^2_{i,l}]\left(\frac{\partial n_{l,2}}{\partial \xi}\right)_{p,T,n_{k\neq l,2}} = \sum_{l=1}^{N_c} J^1_{i,l}\left(\frac{\partial n_{l,\mathrm{tot}}}{\partial \xi}\right)_{p,T,n_{k\neq l,\mathrm{tot}}}, \qquad i = 1,\ldots,N_c. \tag{10}$$

where

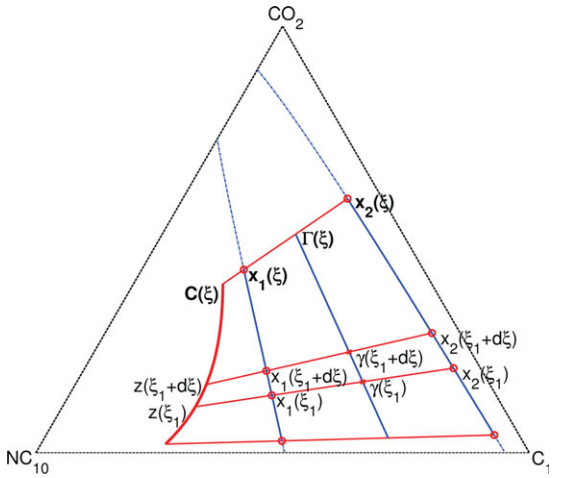

Figure 1. Parameterization continuity for a path, $\mathcal{C}(\xi)$, in the single-phase region.

z and γ are the corresponding points on $\mathcal{C}$ and Γ, respectively. In this example, T = 450 K and p = 180 bar. [Color figure can be viewed in the online issue, which is available at wileyonlinelibrary.com.]

$$J^m_{i,l} = \left(\frac{\partial \mu_{i,m}}{\partial n_{l,m}}\right)_{p,T,n_{k\neq l,m}}, \qquad i,l = 1,\ldots,N_c, \quad m = 1,2. \tag{11}$$

From the Gibbs–Duhem equation we have

$$\sum_{l=1}^{N_c} n_l J^m_{i,l} = 0, \qquad i = 1,\ldots,N_c, \quad m = 1,2. \tag{12}$$

As a result, the righthand side of Eq. 10 is bounded. We note that the solution of the nonlinear set of equations for the phase splitting problem (Eq. 1), whose Jacobian is $\mathbf{J}^1 + \mathbf{J}^2$, is unique. Consequently, the matrix $\mathbf{J}^1 + \mathbf{J}^2$ is invertible, and the differential of $n_{l,2}$ in Eq. 10 is bounded. From Eq. 5 written for the molar amounts and the compositions of each phase, we conclude that the tie-line compositions, $x_{i,j}$, vary continuously along the trajectory.

Next, we generalize the continuity of parameterization along any trajectory. For this purpose, we consider a path, $\mathcal{C}$, in the single-phase region. As the parameterization of the entire compositional space is unique, we define a curve, Γ, within the two-phase region that has an identical parameterization as $\mathcal{C}$ (see Figure 1). Γ is defined as the midpoint locus of a set of tie-lines. We can demonstrate that if $\mathcal{C}$ is continuous, then Γ will be continuous. For this purpose, consider two compositions along $\mathcal{C}$, $\mathbf{z}(\xi_1)$ and $\mathbf{z}(\xi_1 + d\xi)$, that are infinitesimally apart from each other. We need to show that the distance between the corresponding compositions on Γ, $\gamma(\xi_1)$ and $\gamma(\xi_1 + d\xi)$, is finite. Starting from $\gamma(\xi_1)$, we parameterize the straight line between $\gamma(\xi_1)$ and $\gamma(\xi_1 + d\xi)$. Assuming that $d\xi$ is small enough, the line segment is entirely within the two-phase region, and therefore, it has a continuous parameterization. As a result, the midpoint of the parameterizing tie-lines changes continuously, and Γ is continuous. As the parameterizations of $\mathcal{C}$ and Γ are identical, the proof is complete. □

Parameterization in pressure and temperature

Next, we consider a mixture with a fixed overall composition, and we prove the second part of the Continuity Theorem.

Continuity Theorem, Part 2. *At fixed temperature (or pressure), the tie-line that parameterizes a given composition changes continuously with pressure (or temperature).*

Proof: Let us consider changes in pressure. First, we assume that when pressure is changing, the composition remains inside the two-phase region. For a mixture with given overall composition, changing the pressure (at fixed temperature) results in a redistribution of the components between the two phases. Consequently, the chemical potential of a component changes as a function of pressure and component molar amounts. Partial differentiation of Eq. 1 with respect to pressure yields

$$\sum_{l=1}^{N_c}\left(\frac{\partial \mu_{i,1}}{\partial n_{l,1}}\right)_{p,T,n_{k\neq l,1}}\cdot\left(\frac{\partial n_{l,1}}{\partial p}\right)_{T,n_{k\neq l,1}}+\left(\frac{\partial \mu_{i,1}}{\partial p}\right)_{T,n_{k,1}} - \sum_{l=1}^{N_c}\left(\frac{\partial \mu_{i,2}}{\partial n_{l,2}}\right)_{p,T,n_{k\neq l,2}}\cdot\left(\frac{\partial n_{l,2}}{\partial p}\right)_{T,n_{k\neq l,2}}-\left(\frac{\partial \mu_{i,2}}{\partial p}\right)_{T,n_{k,2}}=0, \tag{13}$$

for $i = 1,\ldots,N_c$. Considering that the overall composition (and $n_{i,\mathrm{tot}}$ for each component) is fixed, we differentiate Eq. 8 to obtain

$$\left(\frac{\partial n_{i,1}}{\partial p}\right)_{T,n_{k\neq i,1}}+\left(\frac{\partial n_{i,2}}{\partial p}\right)_{T,n_{k\neq i,2}}=0, \qquad i=1,\ldots,N_c. \tag{14}$$

Combining Eqs. 13 and 14 yields

$$\sum_{l=1}^{N_c}\left[\left(\frac{\partial \mu_{i,1}}{\partial n_{l,1}}\right)_{p,T,n_{k\neq l,1}}+\left(\frac{\partial \mu_{i,2}}{\partial n_{l,2}}\right)_{p,T,n_{k\neq l,2}}\right]\cdot\left(\frac{\partial n_{l,2}}{\partial p}\right)_{T,n_{k\neq l,2}} = \left(\frac{\partial \mu_{i,1}}{\partial p}\right)_{T,n_{k,1}}-\left(\frac{\partial \mu_{i,2}}{\partial p}\right)_{T,n_{k,2}}, \qquad i=1,\ldots,N_c. \tag{15}$$

Using Eq. 11, Eq. 15 simplifies to

$$\sum_{l=1}^{N_c}\left[J^1_{i,l}+J^2_{i,l}\right]\cdot\left(\frac{\partial n_{l,2}}{\partial p}\right)_{T,n_{k\neq l,2}}=\bar{V}_{i,1}-\bar{V}_{i,2}, \qquad i=1,\ldots,N_c, \tag{16}$$

where $\overline{V}_{i,j}$ denotes the partial molar volume of component i in phase j. Similarly, the equilibrium phase amounts of a given mixture at fixed pressure change with temperature as follows

$$\sum_{l=1}^{N_c}\left[J^1_{i,l}+J^2_{i,l}\right]\cdot\left(\frac{\partial n_{l,2}}{\partial T}\right)_{p,n_{k\neq l,2}}=\bar{S}_{i,2}-\bar{S}_{i,1}, \qquad i=1,\ldots,N_c, \tag{17}$$

where the righthand side is the difference between the partial molar entropies of the i-th component. From

$$M_j=\sum_{l=1}^{N_c} n_{l,j}\bar{M}_{l,j}, \qquad j=1,2, \tag{18}$$

we note that the partial molar property of each component ($\bar{M}_{l,j}$) has a finite value. As a result, the derivatives of the molar amounts in Eqs. 16 and 17 are finite, and from Eq. 5, the compositions of parameterizing tie-lines change continuously.

Next, we generalize the continuity of parameterization for a single-phase composition. For this purpose, we consider a curve, Γ, in the two-phase region that (1) has an identical parameterization as the single-phase composition, **z**, and (2) is the midpoint locus of a set of tie-lines. As parameterization of the compositional space is unique at each pressure value, Γ is unique. We show that Γ is a continuous curve, and therefore, the pressure changes continuously along Γ.

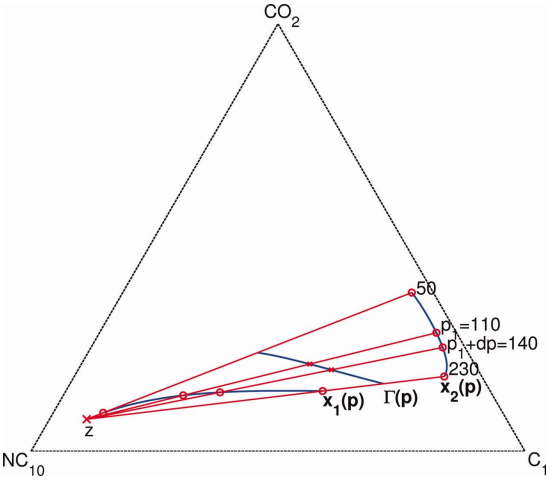

Figure 2. Parameterization in pressure for a single-phase mixture, z.

Numbers show the pressure (in bar) of the tie-lines; for this system, T = 450 K. [Color figure can be viewed in the online issue, which is available at wileyonlinelibrary.com.]

To show the continuity of Γ, consider the midpoint, γ, of the parameterizing tie-line at some pressure value, p_1. We need to demonstrate that $\gamma(p_1+dp)$ is at a finite distance from $\gamma(p_1)$ if dp is small enough (see Figure 2). For this purpose, we first change pressure from p_1 to $p_1 + dp$, then calculate the tie-line that parameterizes $\gamma(p_1)$ at $p_1 + dp$. Assuming that dp is small enough, $\gamma(p_1)$ will remain within the two-phase region, and the midpoint of the resulting tie-line, γ', is at a finite distance from $\gamma(p_1)$. Next, at constant pressure, $p_1 + dp$, we parameterize the straight line connecting γ' to the given mixture, **z**. The parameterization of such a line is continuous, and therefore, $\gamma(p_1 + dp)$ is at a finite distance from γ'. As a result, Γ is a continuous curve (along which pressure changes continuously). As the parameterizations of Γ and the single-phase composition are identical, the proof is complete. Using a similar argument, parameterization of a single-phase composition with temperature at constant pressure is continuous. □

Using numerical experiments, we can show that for a given overall composition at fixed temperature, there is a minimal critical pressure value[18] such that $\mathbf{J}^1 = \mathbf{J}^2$. Noting that $\mathbf{J}^m$ is a singular matrix (see Eq. 12), the tie-lines degenerate to a point. Similar arguments can be made for changes in temperature, or along a trajectory in the compositional space.

Figure 3 describes the parameterization continuity for two-phase, four-component systems. In the first example (see Figure 3a), we show an isothermal table of tie-lines (T = 450 K) for a fixed composition. The mixture is initially in the two-phase region. As the pressure increases, the composition becomes single-phase, and the parameterizing tie-line degenerates at p = 175 bar. We also show how parameterization of the same composition changes with temperature at fixed pressure (see Figure 3b). For this example, the composition is initially single-phase, and it enters the two-phase region as the temperature increases. The parameterizing tie-line becomes critical at T = 550 K.

CSAT

In this section, we describe a generalization of the CSAT framework for systems with an arbitrary number of phases. Then, we present the details of the three-phase CSAT.

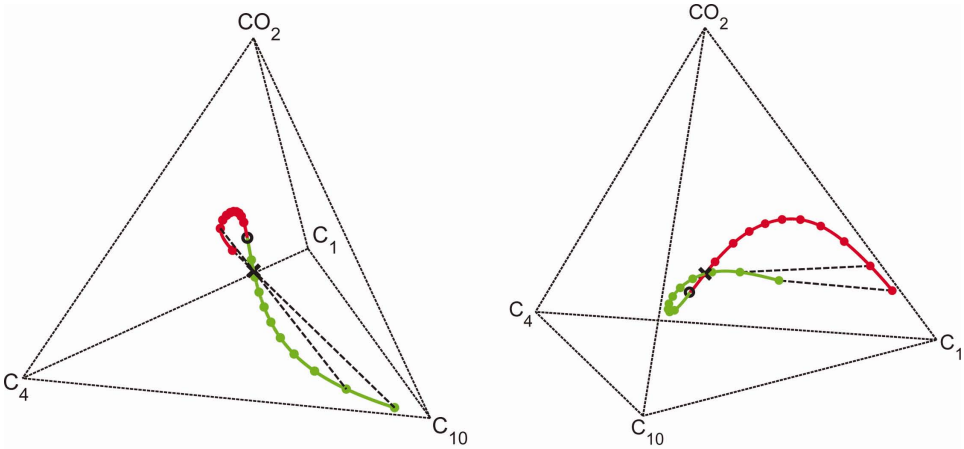

(a) $T = 450$ K, $p = (10, 175)$ *bar* (b) $p = 100$ *bar*, $T = (250, 550)$ K

Figure 3. Continuity of CSP for four-component two-phase systems.

[Color figure can be viewed in the online issue, which is available at wileyonlinelibrary.com.]

Multiphase CSAT

Phase behavior in systems that can form more than two fluid phases is complicated because a large number of regions with two or more phases may be present (see Figure 4). Here, we describe construction of an N_p-phase base tie-simplex parameterization.

We consider an N_p-phase tie-simplex, Δ^{N_p-1}, in a system that can form a maximum of N_p phases at equilibrium ($N_p > 2$). Starting from each $(m-1)$-face of Δ^{N_p-1}, where $m = 2,\ldots,N_p-1$, an m-phase region is extended throughout the compositional space. Let Γ_f^m represent a hyper-volume in the m-phase region that starts from the f-th $(m-1)$-face of Δ^{N_p-1}. By definition, Γ_f^m is parameterized by Δ^{N_p-1}; that is, any composition on Γ_f^m can be expressed as a linear combination of the vertices of Δ^{N_p-1}. Moreover, Γ_f^m is the locus of the geometric center of a set of tie-simplexes in the m-phase region. From the uniqueness of flash calculations in the m-phase region, Γ_f^m is unique. Also, note that Γ_f^m is a continuous hyper-volume, and its representation requires an $(N_p - m)$-dimensional parameterization.

The total number of Γ_f^ms in an N_p-phase system is given by the binomial coefficient

$$\binom{N_p}{m} = \frac{N_p!}{m!(N_p-m)!}. \tag{19}$$

In a three-phase system, for example, a Γ_f^2 curve is connected to each edge of a tie-triangle (see Figure 4). Similarly, in a four-phase system, a Γ_f^3 curve starts from each face of a tie-tetrahedron. Moreover, each edge of a tie-tetrahedron is connected to a Γ_f^2 surface (see the "Numerical Eamples" section).

In the general CSAT framework, a multiphase table is constructed by parameterizing the multiphase regions around a given overall composition at discrete temperature and pressure values. For each level of the $T-p$ grid, Δ^{N_p-1} is calculated, and all the m-phase regions around Δ^{N_p-1} are parameterized using Γ_f^ms. The multi-stage approach for parameterization is designed such that Γ^{m-1} is calculated after all Γ_f^m hyper-volumes are constructed. Therefore, once the N_p-phase tie-simplex is calculated, the procedure starts with discretizing Γ^{N_p-1} and ends with tabulating tie-lines (Γ^2). The parameterization details at each stage are given in Appendix B. We use a multiphase negative-flash procedure to compute the parameterizing tie-simplexes.[21] As Δ^{N_p-1} for a given mixture changes continuously with temperature and pressure, Γ_f^m is a continuous function of these parameters. Note that Γ_f^m is a continuous hyper-volume, and it is parameterized by Δ^{N_p-1}. Moreover, construction of Γ_f^m is still possible, if Δ^{N_p-1} has degenerated. As a result, parameterizing tie-simplexes for each Γ_f^m proves to be very robust in the general CSAT framework.

From extensive numerical experiments, we can show that the volume of the M_p-phase tie-simplex (Δ^{M_p-1}, where $M_p = 2,\ldots,N_p$) that parameterizes a given mixture approaches zero with changes in pressure or temperature (i.e., Δ^{M_p-1} degenerates to Δ^{M_p-2}). Next, we show that the critical tie-simplexes (Δ^{M_p-2}s) change continuously in the compositional space.

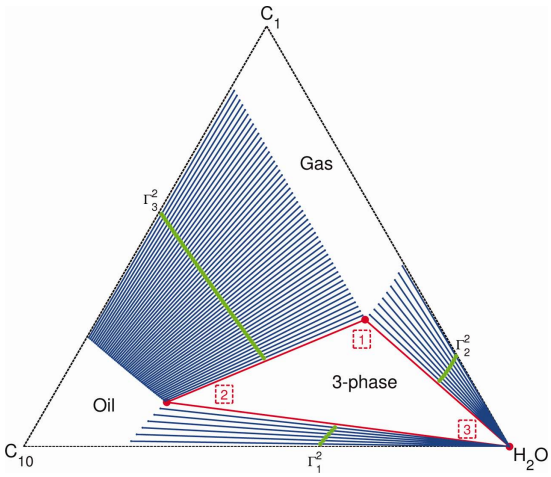

Figure 4. Base tie-simplex parameterization for a three-component system with $N_p^{max} = 3$: complete parameterization of {C_1, C_{10}, H_2O} at $T = 520$ K and $p = 75$ bar using one tie-triangle (in red) and three sets of tie-lines (in blue).

The three Γ^2 curves are shown in green. [Color figure can be viewed in the online issue, which is available at wileyonlinelibrary.com.]

Consider a continuous curve, $\mathcal{C}$, in a compositional space with constant temperature. Let υ denote the volume of a tie-simplex, Δ^{M_p-1}.[20] We assume that $\mathcal{C}$ can be parameterized with a set of tie-simplexes, Δ^{M_p-1}, at different pressure values, such that the volume of each tie-simplex, υ, is a fixed value, ε. Due to the continuity of parameterization, the set of the parameterizing tie-simplexes with volume ε change continuously along $\mathcal{C}$ (also, pressure changes continuously along $\mathcal{C}$). Letting ε be a value close to zero, we conclude the continuity of degenerate tie-simplexes inside the compositional space. For a majority of hydrocarbon systems,[18] the set of degenerate tie-simplexes is unique for the fixed temperature or pressure. In the following sections, we describe two main components of CSAT for three-phase systems.

Parameterization of three-phase compositional space

We start with an overview of the two-phase CSAT Framework.[18] In the natural variable formulation for solving the conservation equations,[6] CSAT provides the accurate number of coexisting phases, as well as an initial guess for EoS-based computations. During iterations, the number of existing phases in each gridblock might change. If the saturation of a phase becomes negative, then the set of the equations are adapted to account for the disappearance of that phase. Furthermore, the phase-state of single-phase gridblocks is checked using the CSAT framework. For multiphase gridblocks, the thermodynamic relations are solved simultaneously with the conservation equations, and upon convergence, the solution route in the compositional space is consistent with phase-state identification of CSAT. Note that a limited number of tie-simplex tables are generated in this formulation. Furthermore, additional negative-flash calculations are performed to resolve the accurate phase-state of mixtures that are too close to the phase boundaries.[18,22]

Given the overall composition of a gridblock, all the tie-line tables are checked to determine if there is any tie-line that parameterizes the composition. The phase-state of the mixture is determined, if its composition and the interpolated tie-line are close enough. Otherwise, a new tie-line table is parameterized and added to the list of tables. For multi-contact miscible displacements, critical tie-lines (at different pressure values) that parameterize the solution path are calculated adaptively and stored. An initial check in the table of critical tie-lines determines if the composition belongs to the supercritical or subcritical regions.

For two-phase systems, a single tie-line parameterizes the two-phase region around a given overall composition. However, for three-phase systems, the entire plane defined by a tie-triangle needs to be parameterized. We can show that this is necessary to guarantee the global minimization of the Gibbs free energy.[22] Note that only a few tie-triangle planes parameterize the solution path in a three-phase compositional displacement.[17,20] Similar to the two-phase CSAT framework, parameterization is performed for mixtures that do not lie on the extension of existing tie-simplex tables. For a given overall composition, we calculate a tie-triangle (Δ^2) and parameterize three curves: Γ_1^2, Γ_2^2, and Γ_3^2. Each one of the Γ^2 curves parameterizes the two-phase behavior on one of the tie-triangle sides.

Here, we demonstrate the construction of a general three-phase thermal-compositional table for a given composition. We assume that the starting pressure at each temperature level is below the minimal degeneration pressure for the three-phase region. For the smallest pressure, the tie-triangle

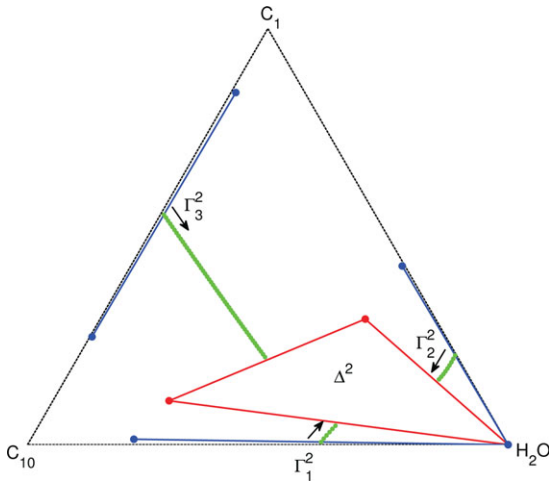

Figure 5. In this example, each Γ_f^2 is parameterized from the farthest composition.

[Color figure can be viewed in the online issue, which is available at wileyonlinelibrary.com.]

that parameterizes the given composition is calculated and stored. Starting from each edge of the tie-triangle, we parameterize the two-phase region by solving for each Γ_f^2 (see Appendix B for the details).

For the next pressure levels, side tie-lines can be calculated toward the tie-triangle. For this purpose, an iterative procedure is used to find the farthest composition on Γ_f^2 at the new pressure level. Parameterization of Γ_f^2 starts from this composition, if the length of the farthest tie-line is greater than the length of the f-th edge of the tie-triangle (see Figure 5). This flexible parameterization framework has proven to be very robust for different three-phase systems over wide ranges of pressure.

As noted previously, the three-phase region degenerates with increase in pressure (see Figure 6). If the pressure is large enough, we solve for the minimal degeneration pressure of the tie-triangle that parameterizes the given composition. An iterative procedure is used to find a pressure value such that the area of the tie-triangle, A, satisfies

$$\varepsilon_{\min} < A < \varepsilon_{\max}, \tag{20}$$

for some small values of $\varepsilon_{\min}$ and $\varepsilon_{\max}$. The plane of the degenerate tie-triangle is then parameterized at higher pressure values. We note that immediately after the degeneration of the tie-triangle, a two-phase region disappears from the plane (see Figure 6a), or the length of a side of the tie-triangle becomes infinitesimal (see Figure 6b). However, all the parameterization techniques developed for subcritical pressures are applicable for higher pressure values.

Tie-lines on a tie-triangle side may also degenerate. For such systems, parameterization of Γ_f^2 is started from the non-degenerate end. Then, we determine how far the parameterization of the tie-lines along Γ_f^2 should proceed until the length of the critical tie-line, ℓ, satisfies

$$\varepsilon_{\min} < \ell < \varepsilon_{\max}, \tag{21}$$

for some small values of $\varepsilon_{\min}$ and $\varepsilon_{\max}$. The calculated critical tie-line marks the boundary between the extendible and non-extendible regions on the f-th tie-triangle side. To obtain the parameterization for a thermal problem, these procedures are performed at discrete temperature levels.

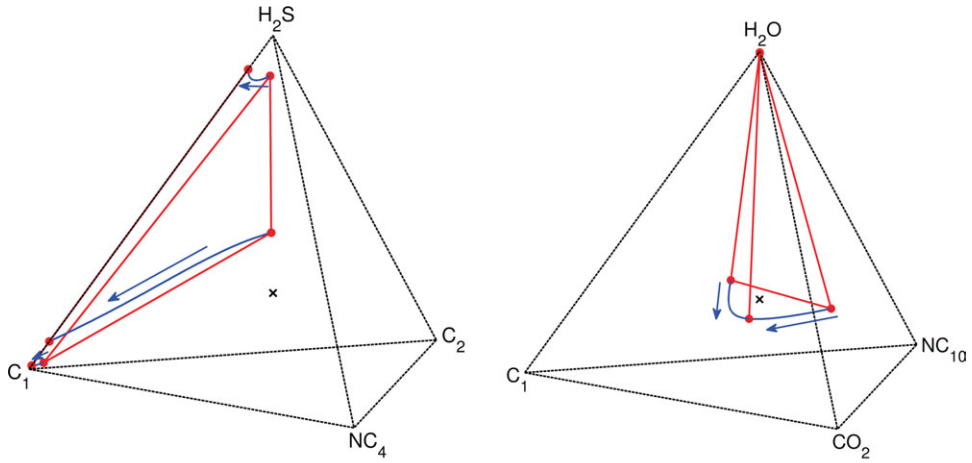

(a) $T = 180\ \mathrm{K}, p = [10, 29.8]\ bar$ (b) $T = 500\ \mathrm{K}, p = [100, 179]\ bar$

Figure 6. Three-phase degeneration patterns, arrows show continuous changes in the tie-triangle compositions from the minimum to the degeneration pressure.

[Color figure can be viewed in the online issue, which is available at wileyonlinelibrary.com.]

Phase-state identification in parameterized compositional space

Based on theoretical considerations from the MoC and extensive flow simulation computations, only a few tables of tie-simplexes are required for a single simulation run.[17,20] In the second stage of the CSAT framework, we use tabulated tie-simplexes to identify the phase-state of mixtures that require phase stability tests.[11]

In the following developments, we assume that a side tie-line lies on the extension of a tie-triangle. The systems that we have considered in our studies exhibit this behavior. We note that CSAT still provides a very good initial guess for conventional phase-behavior calculations in systems that violate this assumption.

Let us consider a thermal three-phase table and describe the procedures for identifying the state of a given composition, $\mathbf{z}$, at some temperature, T, and pressure, p, conditions

$$T_j \le T \le T_{j+1}, \tag{22}$$

$$p_{i_j,j} \le p \le p_{i_j+1,j}, \tag{23}$$

$$p_{i_{j+1},j+1} \le p \le p_{i_{j+1}+1,j+1}, \tag{24}$$

where j denotes the temperature index of the table, and i_j represents the pressure index at the j-th temperature level.

Consider parameterization of the three-phase region in Figure 4. Noting that a Γ curve can be expressed as a linear combination of the tie-triangle compositions, we parameterize Γ_f using fractions of the f-th phase, v_f (see the numbering in Figure 4). We first describe interpolation in tables with identical temperature values. Let N_i^f represent the set of the v_f values for the i-th pressure level. As N_i^f is different from N_{i+1}^f, we initially interpolate tie-lines in v_f to obtain two-phase parameterization for $N_i^f \cup N_{i+1}^f$ at each pressure level. Noting that a composition on Γ_f with a fixed v_f changes continuously with pressure, we interpolate the two sets of side tie-lines in pressure. Performing these interpolations at each temperature level, T_j and T_{j+1}, we finally interpolate in temperature (note that another unification of the v_f values is required). The same interpolation techniques are used after the tie-triangle degeneration pressure.

The tables of tie-simplexes are used to interpolate in temperature and pressure, then $\mathbf{z}$ is projected onto the closest tie-simplexes (see Voskov and Tchelepi[20] and Figure 7). In the general case, $\mathbf{z}$ is in M_p-phase state, if it is inside a Δ^{M_p-1}. Moreover, $\mathbf{z}$ is single-phase, if it is outside all tie-simplexes. These state identification rules are based on the fact that an M_p-phase negative-flash can only determine the state of a mixture in the M_p-phase region.[21]

It is worthwhile to note that a single-phase mixture in a system with $N_p^{\max} = 3$ can be on the extension of:

1. two tie-lines from the same two-phase region (see e.g., Figure 14),
2. two tie-lines from different two-phase regions.

Consider the parameterization of such a mixture. As $N_p^{\max} = 3$, the parameterizing tie-triangle is unique. In the second stage, two-phase regions on the extension of the tie-triangle are parameterized. Unique tie-line parameterization of the Γ^2 curves is still possible because each curve is inside the respective two-phase region, and that tie-lines do not intersect inside the two-phase regions. Moreover, tie-line endpoints change continuously along each Γ^2 curve. This allows for discrete representation of each two-phase region on a side of the tie-triangle.

Next, consider phase-state identification of such a mixture. If it is on the extension of two different tie-lines from the same two-phase region, then the mixture does not lie inside that two-phase region (intersection is possible only outside the multiphase region). Note that for accurate phase-state identification, the boundaries of multiphase regions must be represented correctly. For this purpose, it is sufficient that tie-simplexes do not intersect inside the multiphase regions. Continuity of parameterization is crucial to handle cases with variable temperature and pressure. The boundaries of multiphase regions change continuously with temperature and pressure, and this allows for interpolation in discrete tie-simplex tables.

As noted previously, tie-triangles degenerate differently in various systems. Here, we describe state identification procedures for degenerate steam systems. Consider a three-component steam example at $T = 550$ K (see Figure 8a). The three-phase region becomes critical at $p = 110$ bar. With further increase in pressure, the gas–oil region shrinks until it disappears completely from the plane at $p = 148.9$ bar.

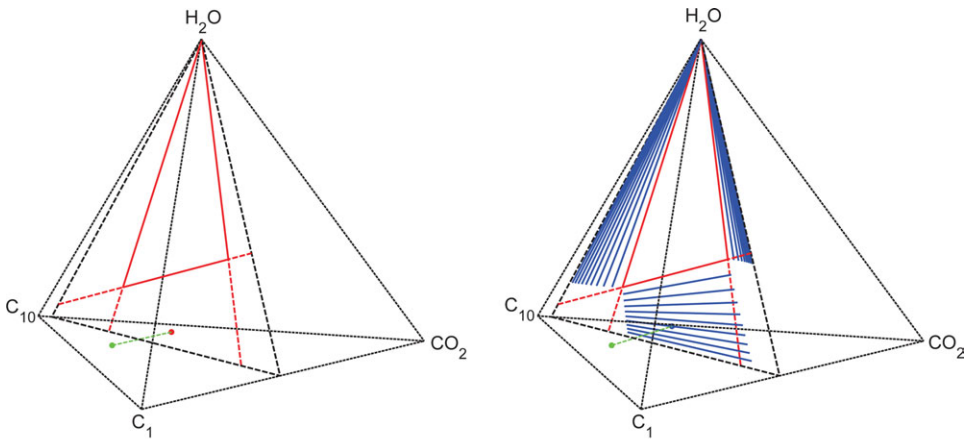

(a) (b)

Figure 7. (a) Projecting a composition onto the plane of tie-triangle and (b) projecting onto a tie-line on the appropriate side of the tie-triangle.

In this example, the state of the composition is identified as two-phase. [Color figure can be viewed in the online issue, which is available at wileyonlinelibrary.com.]

From the continuity of parameterization in degenerate space, the critical gas–oil tie-lines change continuously with pressure. We calculate and store the critical tie-lines at discrete pressure values between the minimal three-phase degeneration pressure and the gas–oil disappearance pressure. Note that the locus of the critical tie-lines is almost linear on the plane of the tie-triangle. The discretized locus of critical tie-lines as well as the critical tie-triangle is then used to identify if a single-phase mixture is gas- or oil-like. This technique is based on the fact that the phase-state of a composition on the extension of a critical tie-line does not change with an increase in pressure.[18] We use this critical boundary to separate water–oil and water–gas tie-lines with an intermediate tie-line, which connects the water phase to a point on the critical tie-line locus (see Figure 8b). If the water tie-lines shrink in size, the critical tie-triangle serves as the intermediate tie-line.

Numerical Examples

In this section, we first present several numerical examples to demonstrate the parameterization techniques for multiphase systems. Next, we show phase-state identification in parameterized steam systems. The computational examples of three-phase thermal-compositional flow simulation are recently presented by Iranshahr et al.[23]

Tie-simplex space parameterization

We show that the generalized CSAT framework accurately captures degeneration of the multiphase regions across a wide pressure range. Parameterization of the three- or two-phase regions can be adaptively refined along pressure or Γ. Typically, this refinement is performed close to a critical tie-simplex.[18]

In an isothermal three-phase table, only two sets of tie-lines parameterize the plane of a degenerate tie-triangle. With further increase in pressure, a two-phase region disappears from the plane. We use an iterative procedure to calculate the pressure at which the two-phase region disappears. That is, we find a pressure value such that the disappearing two-phase region is represented by a trivial tie-line (the

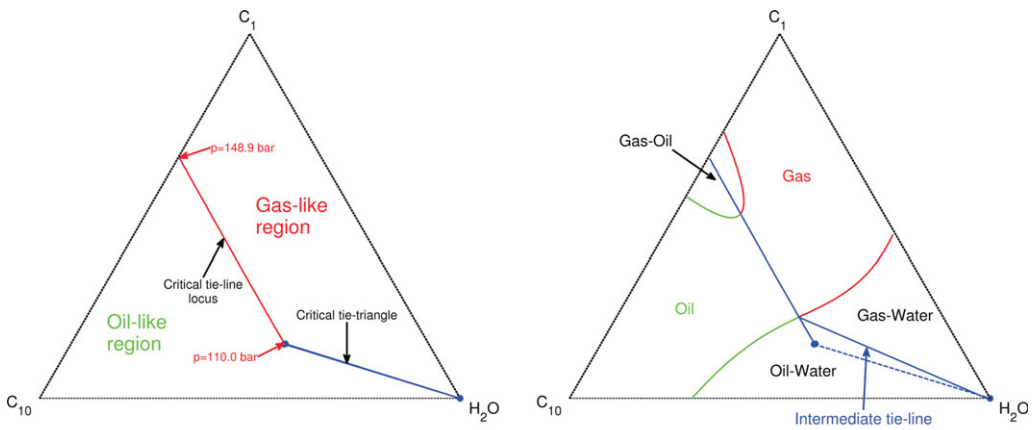

(a) (b)

Figure 8. (a) Critical locus for {C_1, C_{10}, H_2O} at T = 550 K; the locus of critical oil–gas tie-lines is extended from p = 110 to 148.9 bar. (b) Phase behavior at p = 137 bar.

[Color figure can be viewed in the online issue, which is available at wileyonlinelibrary.com.]

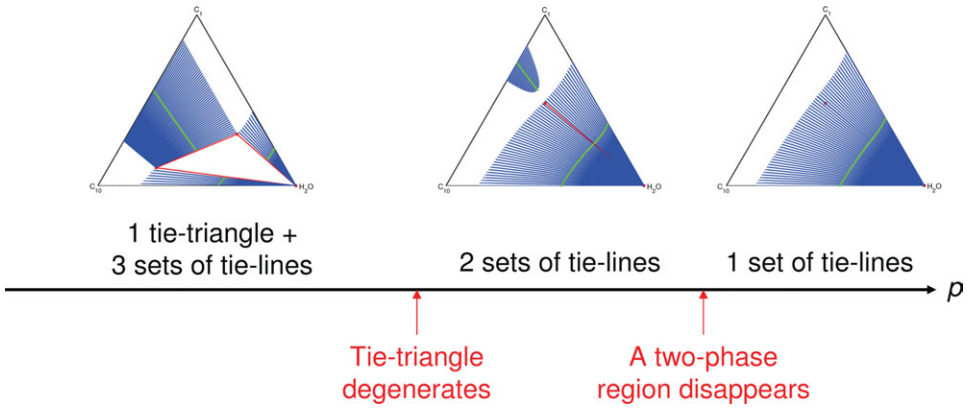

Figure 9. General structure of an isothermal three-phase table.

The three-component systems are calculated at $T = 520$ K and $p = 75$, 180, and 250 bar. [Color figure can be viewed in the online issue, which is available at wileyonlinelibrary.com.]

length of which satisfies Eq. 21). Figure 9 describes the general structure of an isothermal three-phase table.

We validate the accuracy of our numerical results using a reliable commercial simulator.[24] Figure 10 shows the parameterization of a three-component steam system. Using different Equations of State, we also compare the degeneration of the three-phase region (see Figure 11). Note that both equations predict similar three-phase degeneration characteristics.

We describe the three-phase space parameterization for $\{C_1, CO_2, C_{10}, H_2O\}$ at $T = 550$ K. We parameterize the multiphase region for the center of the space (see Figure 12). A three-phase region and three two-phase regions are parameterized for this mixture at $p = 95$ bar. With increase in pressure, the gas–oil side of the tie-triangle becomes critical, and the tie-triangle degenerates to a tie-line at $p = 105.8$ bar. At higher pressure values, the water tie-lines grow in length, and the gas–oil two-phase region shrinks. Here, Γ^2 for the gas–oil region is parameterized from the $\{C_1, C_{10}, CO_2\}$ face. As a result, the associated critical tie-line can be easily captured. Note that after the tie-triangle degeneration pressure, the plane of the degenerate tie-triangle is parameterized (see Figures 12c,d). Also, these examples clearly indicate that the extension of the two-phase tie-lines may intersect inside the compositional space.

Figure 13 shows the full parameterization of the system at $T = 550$ K and $p = 105$ bar. In this system, the three-phase region exists only in a part of the space, and the gas–oil region degenerates close to the $\{H_2O, CO_2, C_{10}\}$ face.

Next, we present three-phase CSP for these systems: (1) a sour gas example: $\{C_1, C_2, H_2S\}$ at $T = 185$ K, Figure 14, and (2) a cold CO_2 example: $\{C_1, C_2, C_6, CO_2\}$ at $T = 180$ K, Figure 15.

Consider two features of the sour gas example. First, the degenerate tie-triangle has three distinct phases; that is, neither of its sides becomes critical. As a result, the Successive Substitution Iterations for the three-phase negative-flash converge faster near the degeneration pressure.[21] Second, tie-lines on a side of the tie-triangle become critical before degeneration of the three-phase region. For this case, Γ^2 is parameterized from the side of the tie-triangle.

Parameterization of four-phase systems is significantly more complicated than three-phase problems. Figures 16 and 17 present the base parameterization of a four-component system with $N_p^{max} = 4$. Here, we first calculate the tie-tetrahedron that parameterizes a given composition. Four curves, Γ^3, parameterize the three-phase regions around the tie-tetrahedron (see Figure 16). Moreover, different two-phase regions in the system are calculated using six surfaces, Γ^2 (see Figure 17). This way, all the multiphase regions on the extension of the tie-tetrahedron are parameterized.

State identification

Here, we demonstrate the accuracy of phase-state identification for several steam systems. Consider the three-component steam example in Figure 10. We choose two compositions and use CSAT to identify the state of the compositions along the dilution line (see Figure 18a). For the first composition, CSAT constructs a three-phase table as described earlier. The phase-state of all the compositions are then determined using this table. Note that a single table parameterizes the entire three-component system. Two- or three-phase compositions are parameterized by a tie-line or tie-triangle, respectively. A single-phase composition is outside all tie-lines and the tie-triangle. Additional two- or three-phase negative-flash calculations may be required to accurately identify the phase-state of mixtures that are too close to the phase boundaries.[18]

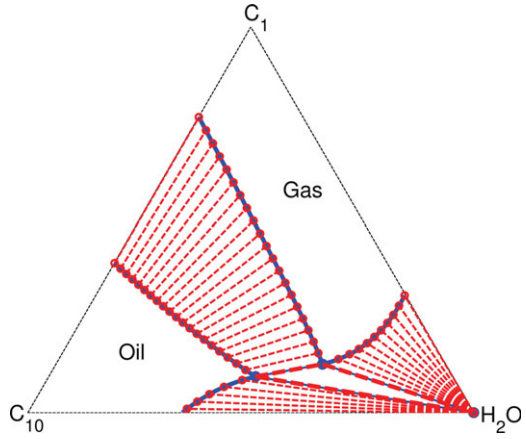

Figure 10. Full parameterization of $\{C_1, C_{10}, H_2O\}$ at $T = 550$ K and $p = 100$ bar.

Compare the phase diagrams in blue with the standard calculations (red tie-lines). [Color figure can be viewed in the online issue, which is available at wileyonlinelibrary.com.]

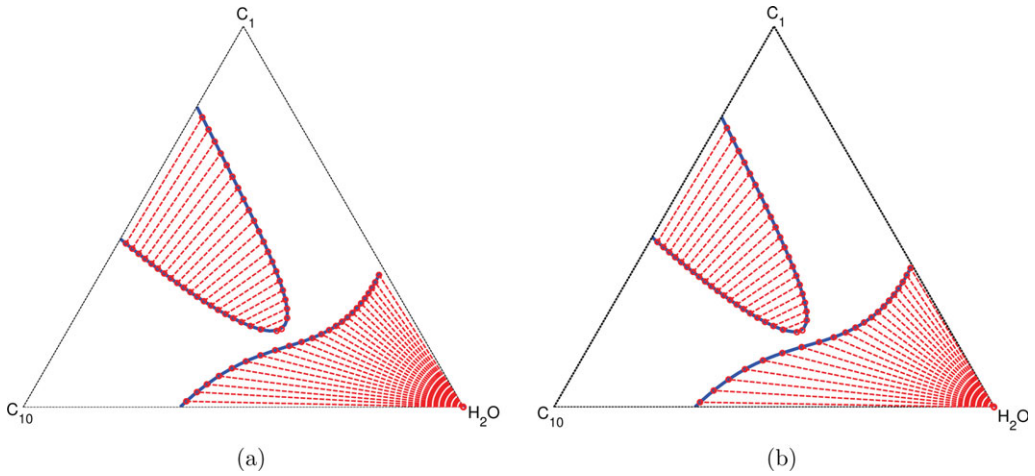

Figure 11. Parameterization of {C_1, C_{10}, H_2O} at $T = 550$ K and $p = 113.8$ bar.

Here, only two sets of tie-lines parameterize the space. The calculations are performed using (a) the SRK-EoS, tie-triangle degenerates at $p = 106.8$ bar and the oil–gas region disappears at $p = 163.5$ bar, and (b) the PR-EoS, tie-triangle degenerates at $p = 110.0$ bar and the oil–gas region disappears at $p = 148.9$ bar. Compare the phase diagrams in blue with the standard calculations (red tie-lines). [Color figure can be viewed in the online issue, which is available at wileyonlinelibrary.com.]

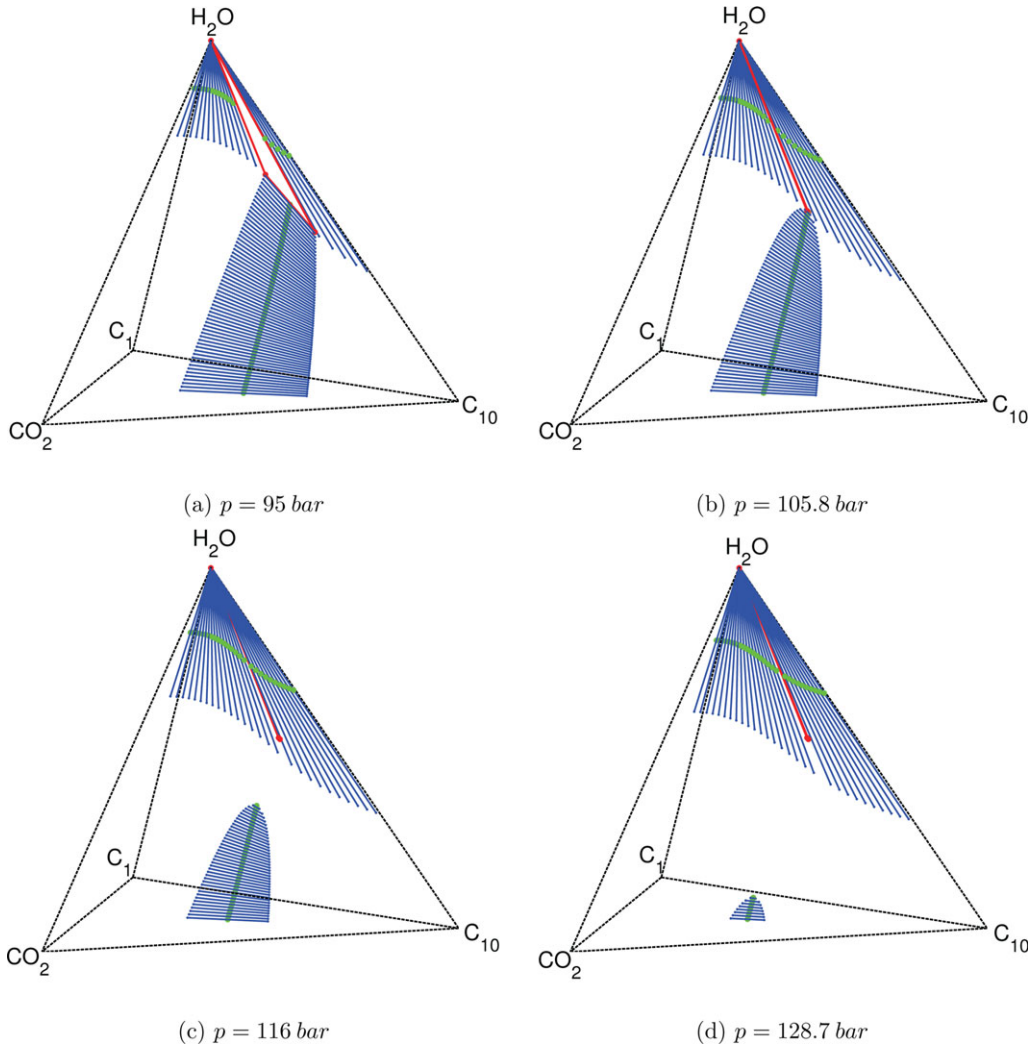

Figure 12. Parameterization of {C_1(0.25), CO_2(0.25), C_{10}(0.25), H_2O(0.25)} at $T = 550$ K.

Tie-triangle degenerates at $p = 105.8$ bar. [Color figure can be viewed in the online issue, which is available at wileyonlinelibrary.com.]

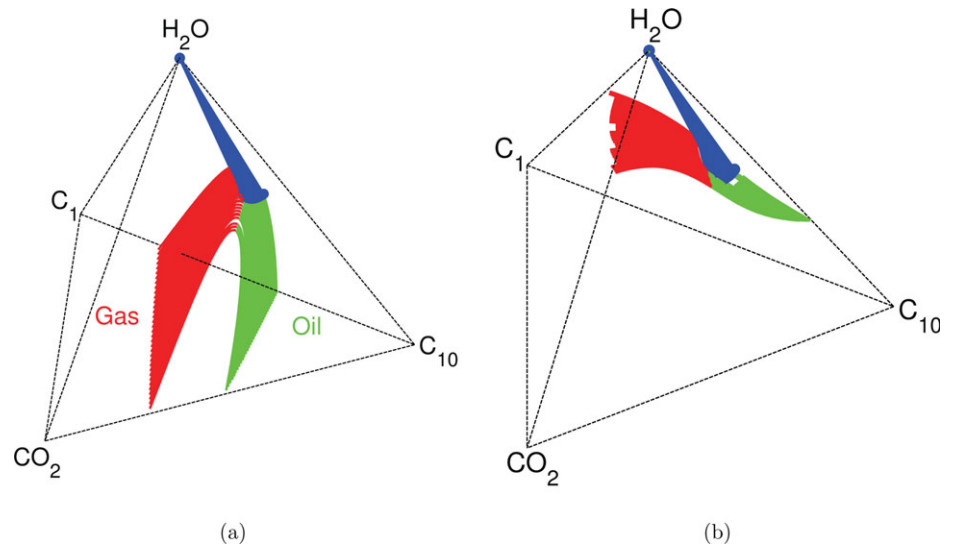

Figure 13. Two views from the full parameterization of {C_1, CO_2, C_{10}, H_2O} at T = 550 K and p = 105 bar: (a) oil–gas tie-lines and (b) water tie-lines.

The three-phase region is enclosed by the blue tie-triangles. [Color figure can be viewed in the online issue, which is available at wileyonlinelibrary.com.]

With increase in pressure, the three-phase region degenerates, and the gas–oil region exhibits critical behavior (see Figure 18b). Here, we also use CSAT to determine the phase-state of a dilution line. Note that the locus of the critical tie-lines, which are at different pressures, separates single-phase gas and oil compositions (see Figure 8).

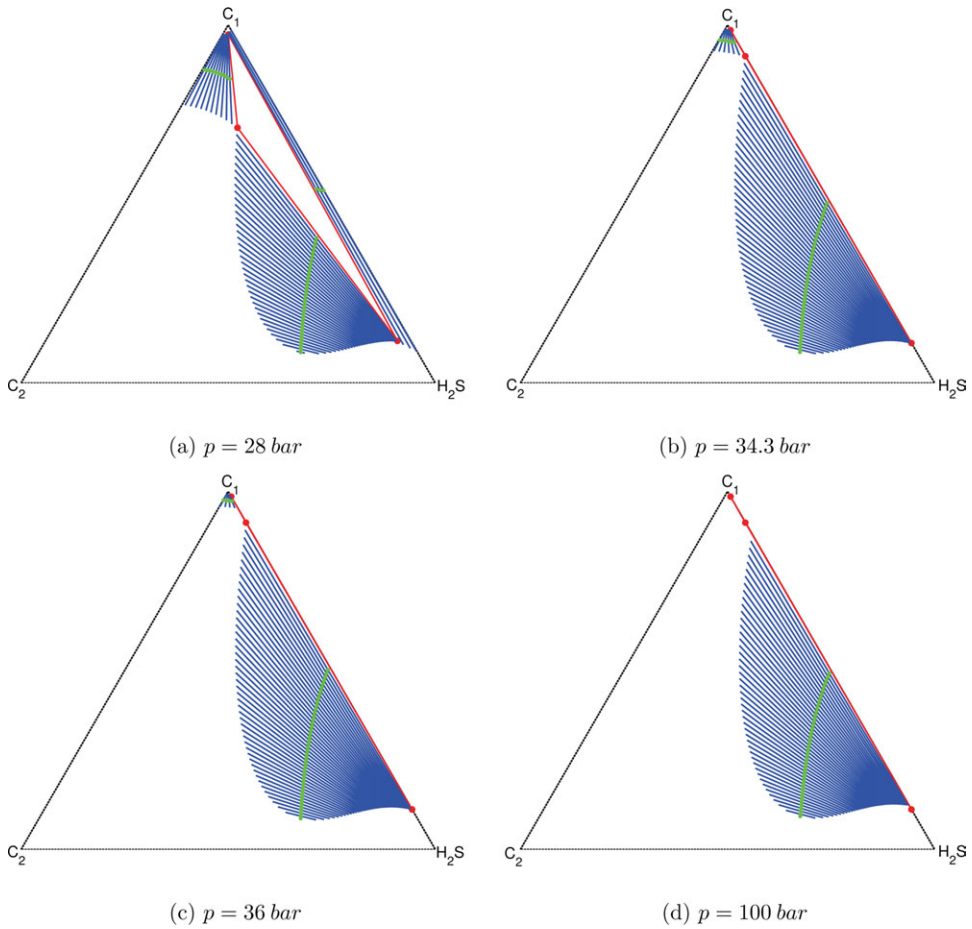

Figure 14. Parameterization of {C_1(0.33), C_2(0.33), H_2S(0.34)} at T = 185 K.

The parameterizing tie-triangle degenerates at p = 34.3 bar. [Color figure can be viewed in the online issue, which is available at wileyonlinelibrary.com.]

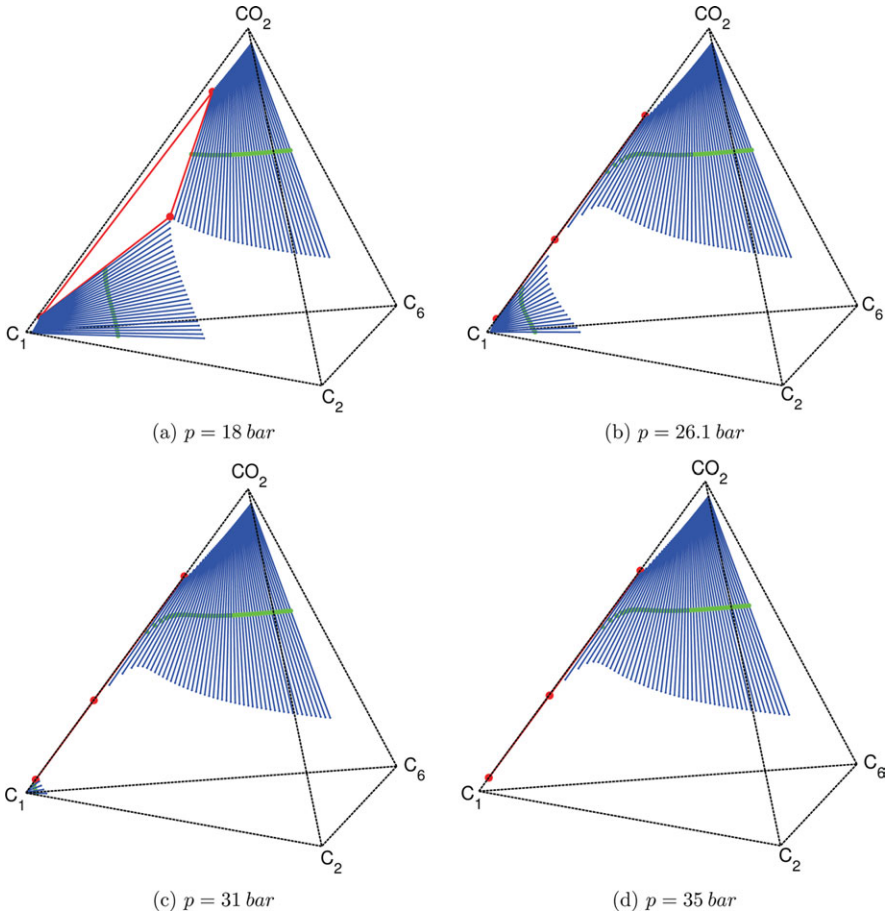

Figure 15. Parameterization of {C_1(0.25), C_2(0.25), C_6(0.25), CO_2(0.25)} at T = 180 K.

The parameterizing tie-triangle degenerates at p = 26.1 bar. [Color figure can be viewed in the online issue, which is available at wileyonlinelibrary.com.]

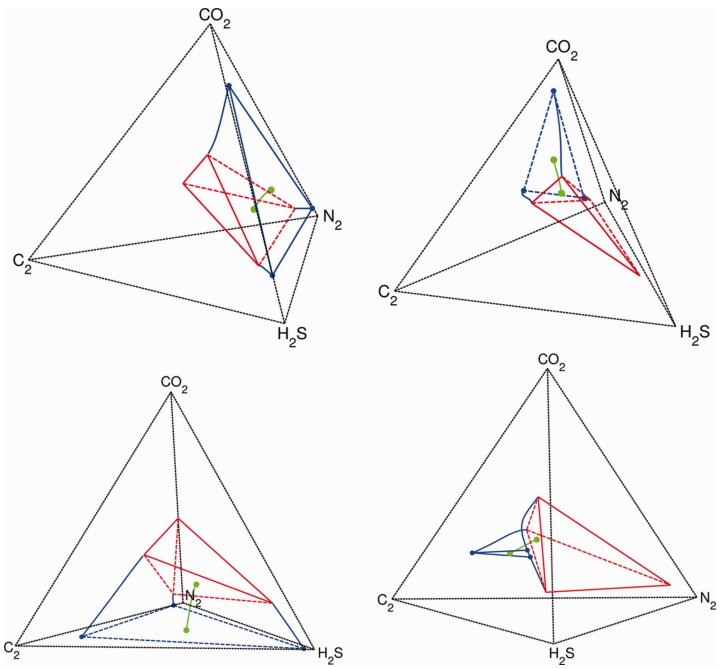

Figure 16. Four Γ^3 curves (in green) that parameterize four different three-phase regions of {C_2, N_2, CO_2, H_2S} at T = 140 K and p = 200 bar.

[Color figure can be viewed in the online issue, which is available at wileyonlinelibrary.com.]

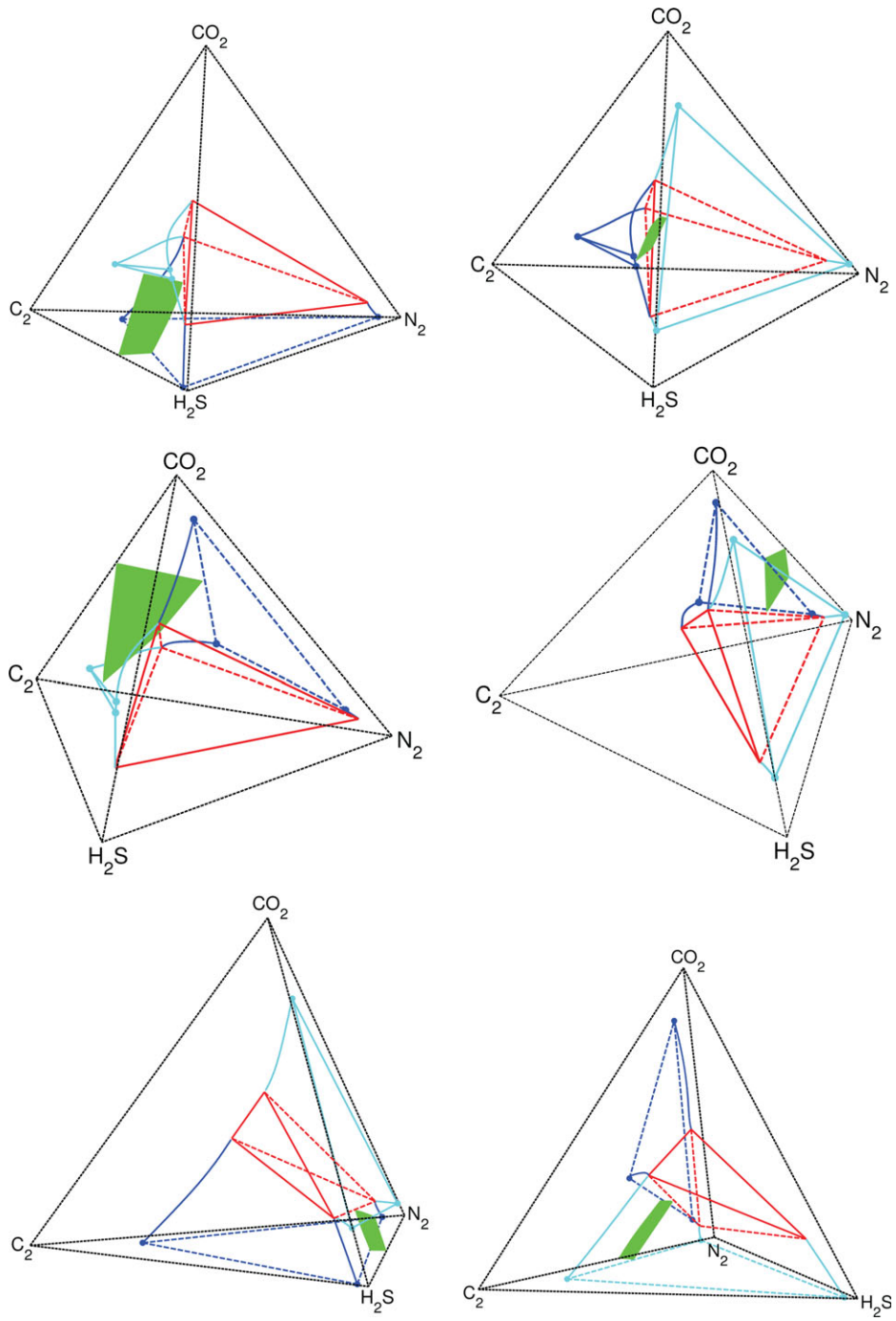

Figure 17. Six Γ^2 surfaces (in green) that parameterize six different two-phase regions of {C_2, N_2, CO_2, H_2S} at T = 140 K and p = 200 bar.

[Color figure can be viewed in the online issue, which is available at wileyonlinelibrary.com.]

Next, we increase pressure for the example in Figure 13 to obtain a fully degenerate steam system (see Figure 19a; it can be considered as a stack of parameterized degenerate planes as shown in Figure 8b). Note that the gas–oil two-phase region exists only in a part of the compositional space. Similarly, we identify the phase-state of the compositions along a dilution line using three-phase CSAT (see Figure 19b). As shown in the figure, only a few parameterized planes are required for this purpose.

Conclusions

We developed the parameterization continuity for the multiphase CSAT framework in general-purpose thermal-compositional simulation. Specifically, we proved that tie-simplex parameterization of any continuous route in the compositional space is continuous. Moreover, the tie-simplex that parameterizes any composition changes continuously with pressure or temperature. We extended the CSAT framework for thermal-compositional systems that can form an arbitrary number of phases. We presented the details of three-phase CSP over wide ranges of pressure. We described phase-state identification procedures for degenerate steam systems. Our numerical examples indicate that CSAT is as reliable as conventional procedures for state identification in multiphase systems, and more importantly, it is very suitable for multiphase EoS-based flow simulation.

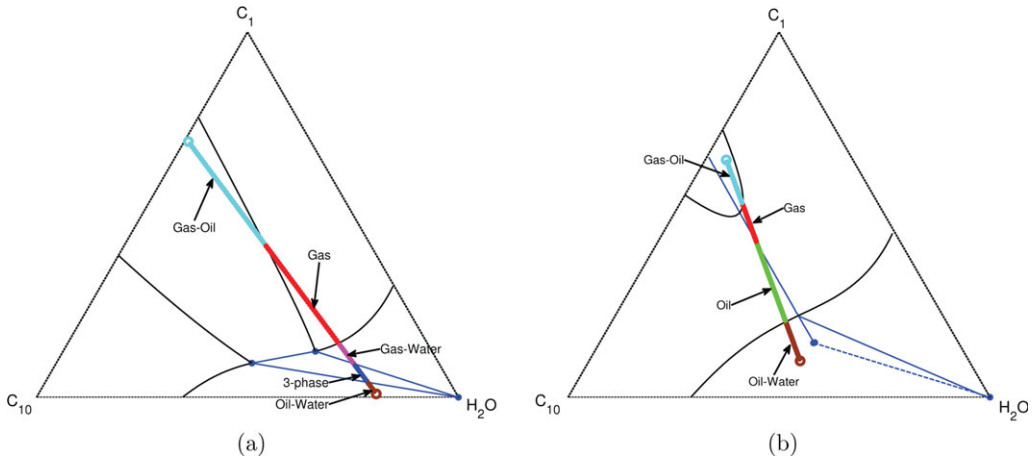

Figure 18. Phase state identification at $T = 550$ K for the dilution line between (a) $\{C_1(0.7),C_{10}(0.29),H_2O(0.01)\}$ and $\{C_1(0.01),C_{10}(0.19),H_2O(0.8)\}$ at $p = 100$ bar, and (b) $\{C_1(0.65),C_{10}(0.3),H_2O(0.05)\}$ and $\{C_1(0.1),C_{10}(0.4),H_2O(0.5)\}$ at $p = 137$ bar.

[Color figure can be viewed in the online issue, which is available at wileyonlinelibrary.com.]

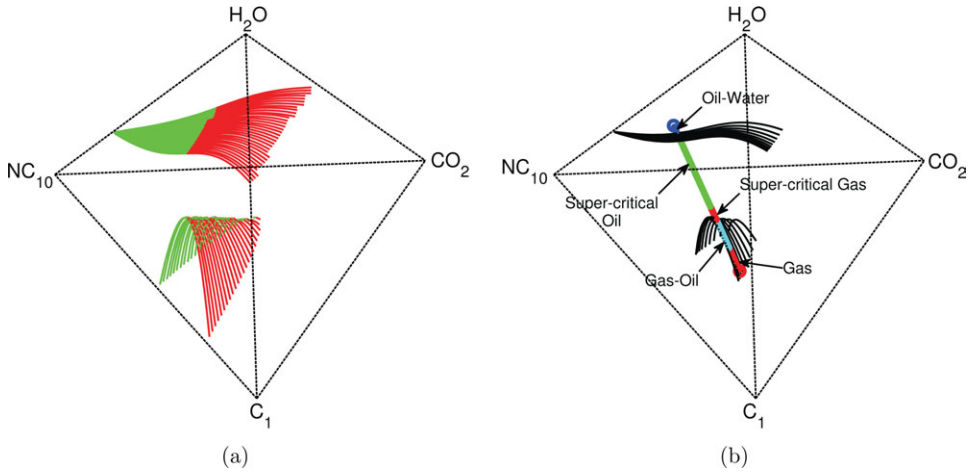

Figure 19. (a) Full parameterization of $\{C_1, CO_2, C_{10}, H_2O\}$ at $T = 550$ K and $p = 137$ bar, and (b) phase state identification for the dilution line between $\{C_1(0.05), C_{10}(0.45), CO_2(0.42), H_2O(0.08)\}$ and $\{C_1(0.47), C_{10}(0.265), CO_2(0.04), H_2O(0.225)\}$.

[Color figure can be viewed in the online issue, which is available at wileyonlinelibrary.com.]

Literature Cited

1. Wong TW, Aziz K. *Considerations in the development of multipurpose reservoir simulation models*. In: *Proceedings of the 1st and 2nd International Forum on Reservoir Simulation*, September 12–16, 1988 and September 4–8, 1989, Alpbach, Austria.
2. Farouq Ali SM, Abou-Kassem J. *Simulation of thermal recovery processes*. In: *Proceedings of the 1st and 2nd International Forum on Reservoir Simulation*, September 12–16, 1988 and September 4–8, 1989, Alpbach, Austria.
3. Bolling JD. *Development and application of a limited-compositional, miscible flood reservoir Simulator*. In: *Proceedings of the SPE Symposium on Reservoir Simulation*, February 1–4, 1987, San Antonio, TX.
4. Whitson CH, da Silva F, Soreide I. *Simplified compositional formulation for modified black-oil simulators*. In: *Proceedings of the SPE Annual Technical Conference and Exhibition*, October 2–5, 1988, Houston, TX.
5. Aziz K, Ramesh AB, Woo PT. Fourth SPE comparative solution project: comparison of steam injection simulators. *J Petroleum Technol*. 1987;39(12):1576–1584.
6. Coats KH. An equation of state compositional model. *SPE J*. 1980;20(5):363–376.
7. Michelsen ML. The isothermal flash problem. Part I. Stability. *Fluid Phase Equilib*. 1982;9(1):1–19.
8. Michelsen ML. The isothermal flash problem. Part II. Phase-split calculation. *Fluid Phase Equilib*. 1982;9(1):21–40.
9. Michelsen ML, Mollerup JM. *Thermodynamic models: Fundamentals & Computational Aspects*. Copenhagen, Denmark: Tie-Line Publications, 2004.
10. Rasmussen CP, Krejbjerg K, Michelsen ML, Bjurstrom KE. Increasing the computational speed of flash calculations with applications for compositional, transient simulations. *SPE Reserv Eval Eng*. 2006;9(1):32–38.
11. Voskov D, Tchelepi H. Compositional space parameterization for miscible displacement simulation. *Transport Porous Media*. 2008; 75(1):111–128.
12. Voskov D, Tchelepi H. Compositional space parameterization: theory and application for immiscible displacements. *SPE J*. 2009; 14(3):431–440.
13. Entov VM. Nonlinear waves in physicochemical hydrodynamics of enhanced oil recovery. *Multicomponent flows*. In: *Proceedings of the International Conference "Porous Media: Physics, Models, Simulations,"* November 19–21, 1997, Moscow, Russia.
14. Orr FM. *Theory of Gas Injection Processes*. Copenhagen, Denmark: Tie-Line Publications, 2007.
15. Zhu J. Multicomponent Multiphase Flow in Porous Media with Temperature Variation or Adsorption PhD Thesis. Stanford, CA: Stanford University, 2003.

16. LaForce TC, Jessen K, Orr FM. Four-component gas/water/oil displacements in one dimension. Part I. Structure of the conservation law. *Transport Porous Media*. 2008;71(2):199–216.
17. LaForce TC, Jessen K, Orr FM. Four-component gas/water/oil displacements in one dimension. Part II. Example solutions. *Transport Porous Media*. 2008;72(1):83–96.
18. Voskov D, Tchelepi H. Compositional space parameterization: multi-contact miscible displacements and extension to multiple phases. *SPE J*. 2009;14(3):441–449.
19. Iranshahr A, Voskov D, Tchelepi H. Tie-simplex parameterization for EoS-based thermal compositional simulation. *SPE J*. 2010; 15(2):545–556.
20. Voskov D, Tchelepi H. Tie-simplex based mathematical framework for thermodynamical equilibrium computation of mixtures with an arbitrary number of phases. *Fluid Phase Equilib*. 2009;283:1–11.
21. Iranshahr A, Voskov D, Tchelepi H. Generalized negative-flash method for multiphase multicomponent systems. *Fluid Phase Equilib*. 2010;299(2):272–284.
22. Iranshahr A, Voskov D, Tchelepi H. Gibbs energy analysis: compositional tie-simplex space. *Fluid Phase Equilib*. 2012;321:49–58.
23. Iranshahr A, Voskov D, Tchelepi H. *A negative-flash tie-simplex approach for multiphase reservoir simulation*. In: *Proceedings of SPE Reservoir Simulation Symposium*, February 21–23, 2011, The Woodlands, TX.
24. Computer Modeling Group. *User's Guide, WinProp Phase Property Program,* Version 2008.

Appendix A: Parameterization Continuity for Systems with an Arbitrary Number of Phases

In this Appendix, we consider the continuity for systems that can form a maximum of N_p phases at equilibrium, where N_p is a predefined number. Let us first consider a continuous trajectory inside the N_p-phase region and study how the parameterizing tie-simplexes (denoted by Δ^{N_p-1}) change along the path at constant temperature and pressure. The equality of chemical potentials for each component between every pair of phases defines a tie-simplex

$$\mu_{i,1} = \mu_{i,j}, \qquad i = 1,\ldots,N_c, \qquad j = 2,\ldots,N_p. \tag{A1}$$

Differentiating Eq. A1 with respect to a parameter along the path, ξ, at constant temperature and pressure yields

$$\sum_{l=1}^{N_c} J_{i,l}^1 \left(\frac{\partial n_{l,1}}{\partial \xi}\right)_{p,T,n_{k\neq l,1}} = \sum_{l=1}^{N_c} J_{i,l}^j \left(\frac{\partial n_{l,j}}{\partial \xi}\right)_{p,T,n_{k\neq l,j}}, \quad i = 1,\ldots,N_c, \quad j = 2,\ldots,N_p, \tag{A2}$$

where $J_{i,l}$ for each phase j is defined by Eq. 11. We consider splitting of each component among all N_p phases

$$n_{i,\mathrm{tot}} = \sum_{m=1}^{N_p} n_{i,m}, \qquad i = 1,\ldots,N_c. \tag{A3}$$

Therefore

$$\left(\frac{\partial n_{i,\mathrm{tot}}}{\partial \xi}\right)_{p,T,n_{k\neq i,\mathrm{tot}}} = \left(\frac{\partial n_{i,1}}{\partial \xi}\right)_{p,T,n_{k\neq i,1}} + \sum_{m=2}^{N_p} \left(\frac{\partial n_{i,m}}{\partial \xi}\right)_{p,T,n_{k\neq i,m}} \tag{A4}$$

Combining Eqs. A2 and A4, and noting that

$$\left(\frac{\partial n_{l,j}}{\partial \xi}\right)_{p,T,n_{k\neq l,j}} = \sum_{m=2}^{N_p} \delta_{j,m} \left(\frac{\partial n_{l,m}}{\partial \xi}\right)_{p,T,n_{k\neq l,m}} \tag{A5}$$

we obtain

$$\sum_{l=1}^{N_c} \sum_{m=2}^{N_p} \left[J_{i,l}^1 + \delta_{j,m} J_{i,l}^j\right] \left(\frac{\partial n_{l,m}}{\partial \xi}\right)_{p,T,n_{k\neq l,m}} = \sum_{l=1}^{N_c} J_{i,l}^1 \left(\frac{\partial n_{l,\mathrm{tot}}}{\partial \xi}\right)_{p,T,n_{k\neq l,\mathrm{tot}}} \tag{A6}$$

where $i = 1,\ldots,N_c$, $j = 2,\ldots,N_p$. As the multiphase flash problem for N_p phases (Eq. A1) has a unique solution (N_p-phase tie-simplexes do not intersect), the Jacobian of Eq. A6 is invertible. Moreover, because the righthand side of Eq. A6 is bounded, the partial derivatives of $n_{l,m}$ are bounded, and from Eq. 5, the equilibrium compositions change continuously.

Next, let us consider a continuous trajectory, $\mathcal{C}$, that is outside the N_p-phase region. As parameterization of the compositional space using N_p-phase tie-simplexes is unique, we can define a curve, Γ, inside the N_p-phase region that has an identical parameterization as $\mathcal{C}$. We also define Γ to be the center of a set of N_p-phase tie-simplexes (hence, Γ is unique). Similar to the two-phase case, one can conclude that Γ is continuous if $\mathcal{C}$ is continuous, and consequently, parameterization along $\mathcal{C}$ (using N_p-phase tie-simplexes) is continuous.

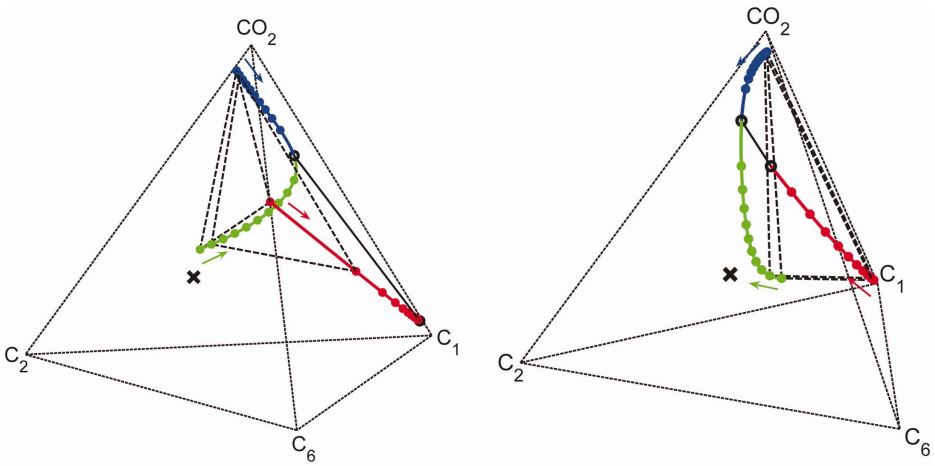

(a) $T = 180$ K, $p = (1, 18.5)$ *bar* (b) $p = 5$ *bar*, $T = (150, 202.9)$ K

Figure A1. Continuity of CSP for four-component three-phase systems.

[Color figure can be viewed in the online issue, which is available at wileyonlinelibrary.com.]

Continuity of multiphase CSP can be shown for changes in pressure or temperature. For this purpose, we consider a mixture with a fixed overall composition and determine how the parameterizing N_p-phase tie-simplexes change with pressure, or temperature. Initially, we assume that the mixture remains inside the N_p-phase region with changes in pressure or temperature. It can be shown that the molar amounts change with respect to p or T as follows

$$\sum_{l=1}^{N_c}\sum_{m=2}^{N_p}\left[J_{i,l}^{1}+\delta_{j,m}J_{i,l}^{j}\right]\left(\frac{\partial n_{l,m}}{\partial p}\right)_{T,n_{k\neq l,m}}=\bar{V}_{i,1}-\bar{V}_{i,j}, \qquad \text{(A7)}$$

$$\sum_{l=1}^{N_c}\sum_{m=2}^{N_p}\left[J_{i,l}^{1}+\delta_{j,m}J_{i,l}^{j}\right]\left(\frac{\partial n_{l,m}}{\partial T}\right)_{p,n_{k\neq l,m}}=\bar{S}_{i,j}-\bar{S}_{i,1}, \qquad \text{(A8)}$$

for $i = 1,\ldots,N_c$ and $j = 2,\ldots,N_p$. Equations A7 and A8 indicate that the partial derivatives of $n_{l,m}$ are bounded; as a result, the parameterizing tie-simplexes change continuously with p or T.

Continuity of parameterization in pressure and temperature can be generalized to any composition. Consider a mixture, $\mathbf{z}$, outside the N_p-phase region. Let Γ be a curve within the N_p-phase region that (1) has an identical parameterization as $\mathbf{z}$ and (2) is the center of a set of N_p-phase tie-simplexes. As parameterization of the compositional space using N_p-phase tie-simplexes is unique at each pressure value, Γ is unique. It can be shown that Γ is a continuous curve (see the similar arguments for the two-phase case), and the parameterization of $\mathbf{z}$ in p (or T) is continuous. Figure A1 shows the continuity of three-phase CSP (in pressure and temperature) for a four-component system.

Appendix B: Discretization of Γ_f^m

Here, we describe the discretization of Γ_f^m on the f-th $(m-1)$-face of an N_p-phase tie-simplex, Δ^{N_p-1} (N_p represents the maximum number of coexisting phases). A similar approach is presented by Voskov and Tchelepi,[20] but it is limited to the parameterization of a tie-triangle plane.

Starting from the center of an m-phase tie-simplex, Δ^{m-1}, we solve for the new points that are farther by a given distance, d. We note that the center of Δ^{m-1}, $\mathbf{a}$, lies on Γ_f^m. Moreover, the vertices of Δ^{m-1} may not be parameterized by Δ^{N_p-1}.

Let $\mathbf{x}_j$ represent the compositions of the j-th vertex of Δ^{N_p-1}, where $j = 1,\ldots,N_p$. We also use $\mathbf{y}_j$ to represent the j-th vertex of Δ^{m-1}, where $j = 1,\ldots,m$. The new composition, $\mathbf{b}$,

1. is parameterized by Δ^{N_p-1},
2. satisfies $(\mathbf{b}-\mathbf{a})\cdot(\mathbf{y}_1-\mathbf{y}_j)=0$ for $j = 2,\ldots,m$,
3. satisfies $\|\mathbf{b}-\mathbf{a}\|_2 = d$, where d is a measure of the separation between two adjacent Δ^{m-1}s.

First, we express $\mathbf{b}$ as a linear combination of the vertices of Δ^{N_p-1}

$$\mathbf{b}=\sum_{j=1}^{N_p}v_j\mathbf{x}_j=\mathbf{X}\boldsymbol{v} \qquad \text{(B1)}$$

where $\mathbf{X}$ is an $N_c \times N_p$ matrix of the vertices of Δ^{N_p-1}, and $\boldsymbol{v}$ is an $N_p \times 1$ vector of the phase fractions. From

$$(\mathbf{b}-\mathbf{a})\cdot(\mathbf{y}_1-\mathbf{y}_j)=0, \qquad j=2,\ldots,m, \qquad \text{(B2)}$$

we write

$$\mathbf{Y}\mathbf{b}=\mathbf{Y}\mathbf{a} \qquad \text{(B3)}$$

where $\mathbf{Y}$ is an $(m-1)\times N_c$ matrix

$$\mathbf{Y}=\begin{bmatrix} y_{1,1}-y_{1,2} & y_{2,1}-y_{2,2} & \cdots & y_{N_c,1}-y_{N_c,2} \\ y_{1,1}-y_{1,3} & y_{2,1}-y_{2,3} & \cdots & y_{N_c,1}-y_{N_c,3} \\ \vdots & \vdots & \vdots & \vdots \\ y_{1,1}-y_{1,m} & y_{2,1}-y_{2,m} & \cdots & y_{N_c,1}-y_{N_c,m} \end{bmatrix}. \qquad \text{(B4)}$$

After combining Eqs. B1 and B3 and adding $\sum_j v_j = 1$ to the set of equations, we obtain

$$\underbrace{\mathbf{B}}_{m\times N_p}\underbrace{\boldsymbol{v}}_{N_p\times 1}=\underbrace{\mathbf{v}}_{m\times 1} \qquad \text{(B5)}$$

where

$$\mathbf{B}=\begin{bmatrix}\mathbf{Y}\mathbf{X}\\ \mathbf{u}\end{bmatrix} \qquad \text{(B6)}$$

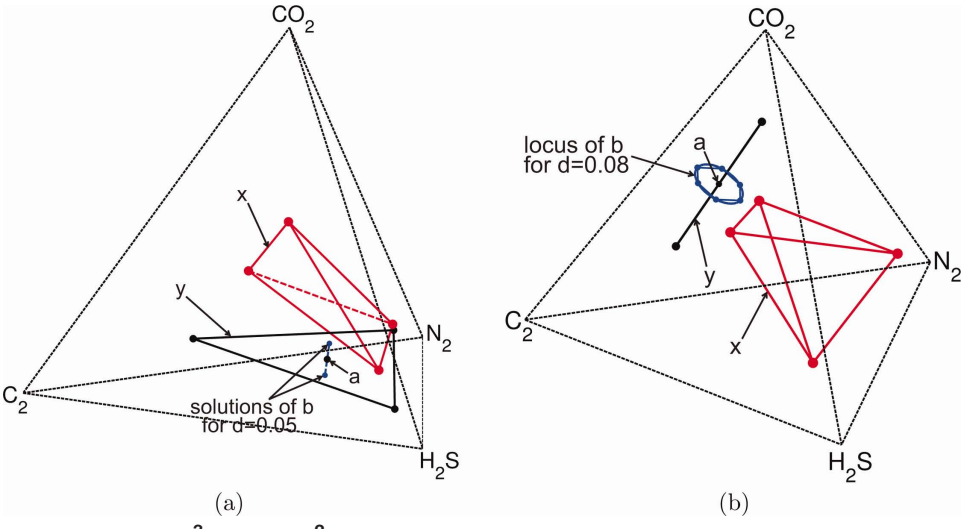

Figure B1. Discretizetion of (a) Γ^3 and (b) Γ^2 for a system with $N_c = 4$ and $N_p = 4$.

[Color figure can be viewed in the online issue, which is available at wileyonlinelibrary.com.]

$$\mathbf{v} = \begin{bmatrix} \mathbf{Ya} \\ 1 \end{bmatrix} \tag{B7}$$

and $\mathbf{u}$ is the $1 \times N_p$ vector of ones. We express $\mathbf{B}$ and $\boldsymbol{v}$ as

$$\mathbf{B} = \begin{bmatrix} \mathbf{B}_1 & \dots & \mathbf{B}_{N_p-m} & \mathbf{B}' \end{bmatrix}, \tag{B8}$$

$$\boldsymbol{v} = \begin{bmatrix} v_1 \\ \vdots \\ v_{N_p-m} \\ \boldsymbol{v}' \end{bmatrix}, \tag{B9}$$

where $\mathbf{B}_j$ is the j-th column of $\mathbf{B}$ ($1 \le j \le N_p-m$). Also, note that $\mathbf{B}'$ is an $m \times m$ matrix. Consequently, from Eq. B5

$$\boldsymbol{v}' = \mathbf{B}'^{-1}\mathbf{v} - \sum_{j=1}^{N_p-m} \mathbf{B}'^{-1}\mathbf{B}_j v_j \tag{B10}$$

We write $\mathbf{X}$ as

$$\mathbf{X} = \begin{bmatrix} \mathbf{X}_1 & \dots & \mathbf{X}_{N_p-m} & \mathbf{X}' \end{bmatrix}. \tag{B11}$$

Similarly, $\mathbf{X}_j$ is the j-th column of $\mathbf{X}$ ($1 \le j \le N_p - m$), and $\mathbf{X}'$ is an $N_c \times m$ matrix. From Eqs. B1 and B10

$$\begin{aligned} \mathbf{b} &= \mathbf{X}'\mathbf{B}'^{-1}\mathbf{v} + \sum_{j=1}^{N_p-m} \left(\mathbf{X}_j - \mathbf{X}'\mathbf{B}'^{-1}\mathbf{B}_j\right) v_j \\ &= \underbrace{\mathbf{P}}_{N_c \times 1} + \sum_{j=1}^{N_p-m} \underbrace{\mathbf{Q}_j}_{N_c \times 1} v_j, \end{aligned} \tag{B12}$$

which indicates that $\mathbf{b}$ is a function of $N_p - m$ phase fractions (Γ_f^m requires an $(N_p - m)$-dimensional parameterization). Finally, from

$$\|\mathbf{b} - \mathbf{a}\|_2 = d, \tag{B13}$$

one can obtain the governing equation for the set of solutions.

If $m = N_p - 1$, Eq. B13 has only two solutions (see Figure B1a). When $m < N_p - 1$, there are an infinite number of solutions for the given d. Only a limited number of them would be required for discrete parameterization (Figure B1b). For this purpose, a generic multidimensional discretization technique can be applied. We use Algorithm 1 to obtain a composition that lies on Γ_f^m.

Algorithm 1. Solving for a composition on Γ_f^m

1: Obtain **b** from Eq. B13
2: **loop**
3: **if** **b** is inside higher-dimensional tie-simplex, or outside compositional space **then**
4: **return**
5: **end if**
6: $\Delta^{m-1} \leftarrow m$-phase negative-flash for **b**
7: **if** Δ^{m-1} is critical **then**
8: $d \leftarrow d/2$
9: Go to Step 1
10: **end if**
11: $\gamma \leftarrow$project geometric center of Δ^{m-1} onto Δ^{N_p-1}
12: **if** γ is close enough to **b** **then**
13: **return** γ
14: **end if**
15: **b** $\leftarrow \gamma$
16: **end loop**

Appendix C: Thermodynamic Parameters of Mixtures

All the calculations in this article are performed using the Peng–Robinson EoS (unless otherwise mentioned). Tables C1–C5 present the thermodynamic parameters of each system.

Table C1. Thermodynamic Parameters for Figures (1–3)

Component	T_c (K)	p_c (bar)	ω	δ_{CO_2}	$\delta_{NC_{10}}$	δ_{C_1}	δ_{C_4}
CO_2	304.2	73.765	0.225	0	0.11	0.103	0.13
NC_{10}	617.6	21.076	0.49	0.11	0	0.052194	0.012228
C_1	190.6	46.00	0.008	0.103	0.052194	0	0.014749
C_4	425.2	38.00	0.193	0.13	0.012228	0.014749	0

Table C2. Thermodynamic Parameters for Figures 4, 5, 6b, 7–13, 18, and 19

Component	T_c (K)	p_c (bar)	ω	δ_{C_1}	$\delta_{NC_{10}}$	δ_{H_2O}	δ_{CO_2}
C_1	190.6	46.00	0.008	0	0.052194	0.4907	0.103
NC_{10}	617.6	21.08	0.49	0.052194	0	0.45	0.11
H_2O	647.3	220.48	0.344	0.4907	0.45	0	0.2
CO_2	304.2	73.765	0.225	0.103	0.11	0.2	0

Table C3. Thermodynamic Parameters for Figures 6a and 14

Component	T_c (K)	p_c (bar)	ω	δ_{C_1}	δ_{C_2}	δ_{H_2S}	δ_{NC_4}
C_1	190.6	46.00	0.008	0	0.002689	0.08	0.014749
C_2	305.4	48.84	0.098	0.002689	0	0.07	0.004914
H_2S	373.2	89.37	0.1	0.08	0.07	0	0.06
NC_4	425.2	38.00	0.193	0.014749	0.004914	0.06	0

Table C4. Thermodynamic Parameters for Figures 15 and A1

Component	T_c (K)	p_c (bar)	ω	δ_{C_1}	δ_{C_2}	δ_{CO_2}	δ_{NC_6}
C_1	190.6	46.00	0.008	0	0.002689	0.103	0.02833
C_2	305.4	48.84	0.098	0.002689	0	0.13	0.013842
CO_2	304.2	73.76	0.225	0.103	0.13	0	0.125
NC_6	507.4	29.69	0.296	0.02833	0.013842	0.125	0

Table C5. Thermodynamic Parameters for Figures 16 and 17

Component	T_c (K)	p_c (bar)	ω	δ_{C_2}	δ_{N_2}	δ_{CO_2}	δ_{H_2S}
C_2	305.4	48.84	0.098	0	0.1	0.1	0.07
N_2	126.2	33.94	0.04	0.1	0	0	0.176
CO_2	304.2	73.76	0.225	0.1	0	0	0.096
H_2S	373.2	89.37	0.1	0.07	0.176	0.096	0

Manuscript received Sept. 6, 2011, and revision received May 12, 2012.